FINAL REPORT

NAG5-9508

Analysis of EIT/LASCO Observations Using Available MHD Models: Investigation of CME Initiation Propagation and Geoeffectiveness

Period of Performance: June 1, 2000 – May 31, 2001

By

S. T. Wu
Center for Space Plasma and Aeronomic Research
Department of Mechanical & Aerospace Engineernig
The University of Alabama in Huntsville
Huntsville, AL 35899 USA

During the period of performance (June 1, 2000 – May 31, 2001) of grant NAG5-9508, we have complete the work according to our proposed plan. A paper was published in *IEEE Transactions of Plasma Science*. The highlights of the work are summarized in the following:

The Sun's activity drives the variability of geospace (i.e. near-Earth environment). Observations show that the ejection of plasma from the sun, called coronal mass ejections (CMEs), are the major cause of geomagnetic storms. This global-scale solar dynamical feature of coronal mass ejection was discovered almost three decades ago by the use of space-borne coronagraphs (OSO-7, Skylab/ATM and P78-1). Significant progress has been made in understanding the physical nature of the CMEs. Observations show that these global-scale CMEs have size in the order of a solar radius (~ 6.7×10^5 km) near the Sun, and each event involves a mass of about 10^{15} g and an energy comparable to that of a large flare on the order of 10^{32} ergs. The radial propagation speeds of CMEs have a wide range from tens to thousands of kilometers per second. Thus, the transit time to near Earth's environment (i.e. 1 AU (astronomical unit)) can be as fast as 40 hours to 100 hours. The typical transit time for geoeffective events is ~ 60-80 hrs [1].

We have published our results in the refereed journal IEEE Transactions of Plasma Science. The journal article covers two parts. (i) A summary of the observed CMEs from Skylab to the present SOHO. Special attention was made to SOHO/LASCO/EIT observations and their characteristics leading to a geoeffective CME. (ii) The chronological development of theory and models to interpret the physical nature of this fascinating phenomenon was reviewed. Also, an example was used to illustrate the geoeffectiveness of the CMEs by using both observation and model. Details can be found in the IEEE publication.

Publications

1. Coronal Mass Ejections (CMEs) and Their Geoeffectiveness, S. P. Plunkett and S. T. Wu, *IEEE Transactions of Plasma Science*, 28,(6) 1807-1817, 2000.

Coronal Mass Ejections (CMEs) and their Geoeffectiveness

Simon P. Plunkett and Shi Tsan Wu

Invited Paper

Abstract—**The Sun's activity drives the variability of geospace (i.e., near-earth environment). Observations show that the ejection of plasma from the sun, called coronal mass ejections (CMEs), are the major cause of geomagnetic storms. This global-scale solar dynamical feature of coronal mass ejection was discovered almost three decades ago by the use of space-borne coronagraphs (OSO-7, Skylab/ATM and P78-1). Significant progress has been made in understanding the physical nature of the CMEs. Observations show that these global-scale CMEs have size in the order of a solar radius ($\sim 6.7 \times 10^5$ km) near the sun, and each event involves a mass of about 10^{15} g and an energy comparable to that of a large flare on the order of 10^{32} ergs. The radial propagation speeds of CMEs have a wide range from tens to thousands of kilometers per second. Thus, the transit time to near earth's environment [i.e., 1 AU (astronomical unit)] can be as fast as 40 hours to 100 hours. The typical transit time for geoeffective events is ~60–80 h [1].**

This paper consists of two parts. 1) A summary of the observed CMEs from Skylab to the present SOHO will be presented. Special attention will be made to SOHO/LASCO/EIT observations and their characteristics leading to a geoeffective CME. 2) The chronological development of theory and models to interpret the physical nature of this fascinating phenomenon will be reviewed. Finally, an example will be presented to illustrate the geoeffectiveness of the CMEs by using both observation and model.

Index Terms—**Coronal ejection, MHD modeling, solar activity, sun–earth connection.**

I. Introduction

BEFORE the development of spaceborne white-light coronagraphs about thirty years ago, our knowledge of the solar corona was limited to observations made by a very few ground-based coronagraphs or during total solar eclipses. Our impression was that the corona was a very quiet, almost static, structure similar to that shown in Fig. 1, with a very slow evolution in its appearance over the 11-year solar activity cycle. Now we recognize that the corona is a very dynamic place, with activity occurring over a wide range of temporal and spatial scales. Perhaps the most spectacular manifestation of this activity is the phenomenon known as a coronal mass ejection (CME). These are transient phenomena that involve the expulsion of significant amounts of plasma and magnetic flux from the sun into interplanetary space, with speeds up to a few thousand km/s, on a timescale between a few minutes and several hours. Observations show that the fast interplanetary manifestations of CMEs can drive shocks that accelerate charged particles to high energies and that they are the origin of structures in the solar wind known as magnetic clouds [2]. When they impact on earth, CMEs are the major solar drivers of large, nonrecurrent geomagnetic storms. It is well known that geomagnetic storms have direct adverse effects on high-technology systems, both on the ground and in space. For example, spacecraft problems range from telemetry dropouts and triggering of false commands to permanent loss. During a geomagnetic storm on January 20–21, 1994, two Canadian communications satellites were disabled. The great storm of March 1989 destroyed a Japanese satellite and created severe problems for others. On the ground, during the same storm, the Hydro Quebec electric power grid was disrupted by transient voltage fluctuations that saturated transformers and overheated transmission lines causing power blackouts.

Fig. 1. The solar corona observed during the total eclipse of November 3, 1994 with the High Altitude Observatory's White Light Coronal Camera. North is at the top in this image, and east is at the left. Helmet streamers can be seen on both the east and west limbs. The low-lying parts of these streamers consist of magnetic loops filled with hot coronal gas. The upper parts of these loops are stretched outward by the expanding solar wind, giving the characteristic helmet shape. This image is courtesy of the High Altitude Observatory, National Center for Atmospheric Research (NCAR), Boulder, CO, USA. NCAR is sponsored by the National Science Foundation.

Manuscript received January 10, 2000; revised June 29, 2000. The work of S. T. Wu was supported by NASA under Grant NAG5-9508, the National Science Foundation under Grant ATM 9633629, and the Air Force Office of Scientific Research under Grant F49620-00-0-0204. The work of S. P. Plunkett was supported by NASA under Grant NAG5-8116 and under Contract NAS8-6760E.

S. P. Plunkett is with the Universities Space Research Association, Code 7667, Naval Research Laboratory, Washington, DC 20375 USA.

S. T. Wu is with the Center for Space Plasma and Aeronomic Research and Department of Mechanical Engineering, The University of Alabama, Huntsville, AL 35899 USA.

Publisher Item Identifier S 0093-3813(00)11638-8.

With all these unavoidable adverse effects, and our increasing dependence on high-technology systems in everyday life, a National Space Weather Program was established in the United States to advance our knowledge in solar-terrestrial physics for developing a science-based space weather prediction scheme. One of the major components of this effort is to further our understanding of the geoeffectiveness of CMEs.

In this paper, a survey of observed CME properties from space missions from Skylab to SOHO will be presented to illustrate the general characteristics of CMEs. Special emphasis will be given to the recent SOHO observations of geoeffective CMEs. The chronological development of theory and models to interpret the physical nature of CMEs will be discussed, and an example will be presented to illustrate the geoeffectiveness of a CME by using both observations and modeling.

II. Overview of CME Observations and their Geoeffectiveness

A white-light coronagraph records photospheric light over a broad band of wavelengths that has been scattered by free electrons in the highly ionized coronal plasma. Coronagraph images thus provide information on the plasma density and magnetic field structure (the high degree of ionization means that the plasma is "frozen" to the magnetic field), but are insensitive to other parameters such as temperature. Since the corona is optically thin at visible wavelengths, the brightness at any given location in an image depends on the integral of this scattered light along the line of sight from the telescope. This integral is weighed in favor of scattering by electrons directly over the limb of the sun, with decreasing contributions from electrons located away from the "plane of the sky" [3]. Thus, coronal structures, including transient phenomena such as CMEs, are best observed in a white-light coronagraph when they are located directly above the limb, and features or events that occur well away from the limb are harder to observe in detail.

CMEs were first observed with a coronagraph on the OSO-7 satellite [4]. Since then, thousands of these events have been observed from Skylab [5], [6] P78-1/Solwind [7], the Solar Maximum Mission (SMM) [8]–[10], and more recently the Solar and Heliospheric Observatory (SOHO) [11], [12]. CMEs have also been observed with the ground-based K-coronameter at Mauna Loa Solar Observatory. The frequency of occurrence of CMEs varies by about an order of magnitude in phase with the solar cycle. Near solar maximum, Webb and Howard [13] found a rate of about 3.5 events per day over the whole sun. The typical CME mass is in the range 10^{15} to 10^{16} grams. The speeds measured in coronagraph images range from less than 100 km/s to more than 2000 km/s within about 10 $R_\odot$ from the solar surface ($R_\odot$ is the solar radius, about 6.7×10^5 km). The average speed is about 400 km/s, which is similar to the typical speed of the slow solar wind at 1 AU. The average angular size of CMEs is about 45°. Thus, it is clear that these are truly large-scale phenomena, involving the disruption of a region in the corona that covers a substantial fraction of a solar radius, and the expulsion of the plasma within this region into interplanetary space with kinetic energies on the order of 10^{31} ergs. The masses, speeds, and sizes quoted here are all measured in the image plane or require some assumption about the distribution of the plasma along the line of sight. Projection effects as discussed in the last paragraph are not taken into account, but would usually introduce correction factors of only about 10%.

Near solar minimum, most CMEs occur at low heliographic latitudes near the magnetic equator, but at solar maximum CMEs occur at all locations around the disk. The ejections arise predominantly from large-scale closed magnetic field regions in the solar atmosphere, visible in coronal images such as Fig. 1 as "helmet streamers." Many CMEs begin as a slow swelling or brightening of a streamer [9] and have the appearance of a magnetic loop that connects back to the sun at both ends. Within this loop, a dark void or "cavity" of relatively low density is often observed. A compact bright feature called the "core" is sometimes embedded in the cavity. The variation in CME latitudes over the solar cycle is also similar to that of large-scale solar features such as helmet streamers and prominences (structures containing relatively cool chromospheric material that can remain suspended in the corona for periods up to several weeks before disappearing, often by erupting outwards).

CMEs can be identified in interplanetary space by a number of signatures [14]. These signatures include bidirectional streaming of electrons and protons, low plasma β (the ratio of gas pressure to magnetic pressure), enhanced helium abundance and anomalous abundance of other species, low ion or electron temperatures, and enhanced magnetic field strength and smooth rotation of the field orientation. However, it is rare to find all of these signatures in any one event, and there is no signature that is uniquely present in all events. It is often unclear which parts of the structures observed *in situ* correspond to the features observed with coronagraphs, so the term interplanetary CME (ICME) is often used to distinguish the ejected plasma in the solar wind. A CME that propagates through the interplanetary medium with a speed exceeding the ambient wind speed by the local magnetosonic wave speed will drive a shock ahead of it [15]. CME-driven shocks can effectively accelerate large fluxes of energetic particles from the ambient solar wind [16]. These particles can pose a hazard to spacecraft systems and to humans operating in space. A fast CME will also sweep up and compress slower plasma ahead of it, creating a "sheath" region between the shock and the ejected plasma.

The Large Angle Spectrometric Coronagraph (LASCO) [17] on the ESA/NASA Solar and Heliospheric Observatory (SOHO) has been observing the corona almost continuously since early 1996. LASCO is a suite of three coronagraphs with concentric fields of view. The outer two coronagraphs, designated C2 and C3, are white-light imagers with a combined field of view extending from 2 to 30 $R_\odot$. LASCO also has considerably improved sensitivity and dynamic range over earlier coronagraphs. These improved characteristics allow CMEs to be studied in greater detail than before. Fig. 2 shows a series of images from LASCO C2 that illustrates the development of a CME above the southwest limb on June 2, 1998 [18]. This CME shows the classic three-part structure, with a bright frontal loop, followed by a darker cavity and a bright, twisted

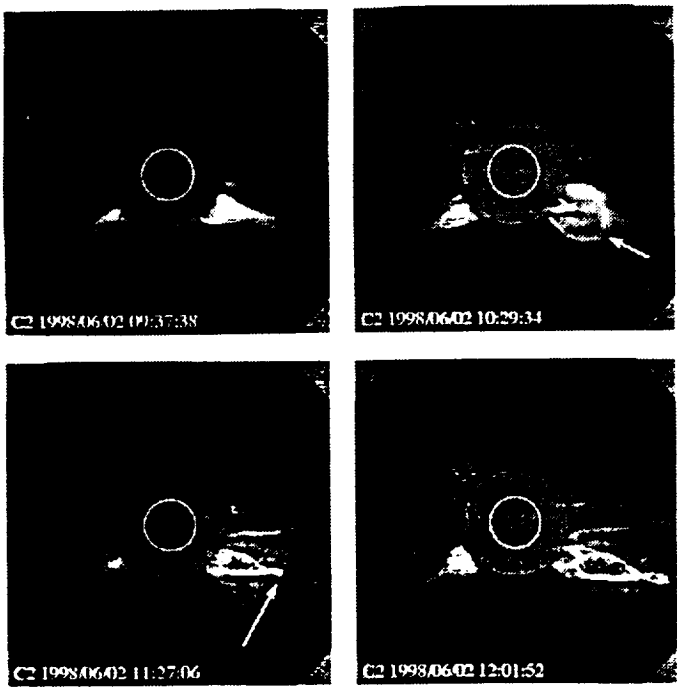

Fig. 2. The CME of June 2, 1998 observed by the LASCO C2 coronagraph on SOHO. The bright frontal loop of the CME is marked by an arrow in the image at 10:29 UT. This is followed by a dark cavity and a bright, twisted prominence. The arrow on the image at 11:27 UT shows the location of concave-outward features near the top of the prominence (see the text for discussion of these features). The white circle represents the sun, and the solid disk is the coronagraph occulter, which extends to about 2 $R_\odot$ (taken from [18]).

core. This twisted structure is cool prominence material that could be observed in the low corona prior to the eruption. A series of concave-outward, bright striations are visible near the top of the prominence, and these striations appear to join with the leading edge to form a closed, almost circular structure. This has been interpreted by Plunkett *et al.* [18] as evidence for a helical magnetic structure called a flux rope. Dere *et al.* [19] estimate that about one third of all CMEs observed by LASCO show similar features. Flux rope signatures are also observed in about one third of CMEs observed *in situ* in interplanetary space [20], where they are often referred to as "magnetic clouds" [2].

In order to impact the earth and cause a geomagnetic disturbance, a CME must be launched along the sun–earth line, or at least close enough to that line so that some part of the ejection intercepts the earth. Since the average CME width is about 45°, it is clear that most geoeffective CMEs must originate well away from the solar limb. Thus, they will be more difficult to observe with a coronagraph and may be expected to have a markedly different appearance to CMEs that occur near the limb. The three-dimensional structure of CMEs is difficult to determine from coronagraph images. Nonetheless, some simple conceptual models to describe their gross characteristics can be constructed. One such model of a CME as a shell-like region of enhanced density is shown in Fig. 3. When such a structure is viewed above the solar limb, it has the loop-like appearance common to many CMEs, but clearly does not reproduce the detailed structure such as shown in Fig. 2. If this

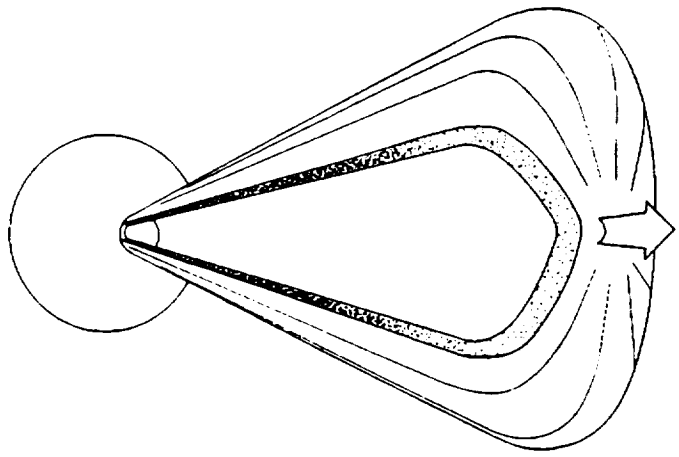

Fig. 3. A conceptual model of a CME as a shell-like region of enhanced density [21].

structure is observed head-on rather than from the side, it would appear as a diffuse ring of enhanced brightness surrounding the sun. Howard *et al.* [21] first described such a "halo of excess brightness surrounding the occulting disk and propagating radially outward in all directions from the sun" in images from the Solwind coronagraph, and they interpreted the observations as evidence of a CME directed toward earth. In total, Solwind detected about thirty events that were classified as either halo or partial halo (where the excess brightness did not extend all the way around the occulting disk) from 1979 to 1983. Only a few partial halo events were identified in the SMM data in 1980 and from 1984 to 1989 [8]. Many more halos have been observed with LASCO, as a direct result of its improved ability to detect faint features. St. Cyr *et al.* [12] performed a detailed study of all CMEs observed by LASCO from January 1996 to April 1998, and concluded that 11% of the events were either halos or partial halos. In other respects, St. Cyr *et al.* [12] found that the observed properties (apparent speeds, occurrence rates, locations and sizes) of LASCO CMEs were very similar to those observed with other coronagraphs.

Even when a halo is identified in coronagraph images, the physics of the scattering process is such that events moving toward the observer cannot be distinguished from events moving away from the observer. Complementary observations of associated activity on the solar disk are required to confirm that a halo CME is indeed directed at earth. Fig. 4 shows a partial halo CME observed by LASCO on January 6, 1997 [22]. This CME appeared as a faint diffuse front moving outward over the South pole in the LASCO images. Its appearance is very different to the highly structured event shown in Fig. 2. This CME was only visible in "running difference" images, where each image has had the previous image in the sequence subtracted, thus highlighting the changes in the coronal scene from one image to the next. This CME was associated with the eruption of a small filament (a prominence seen in projection against the solar disk) just to the south of disk center, in an otherwise quiet region of the sun [23]. Subsequently, a shock and magnetic cloud were observed in interplanetary space near the earth [24] about four days after the launch of the CME from the sun, and a geomagnetic storm occurred around the same time. Unusually, a cool,

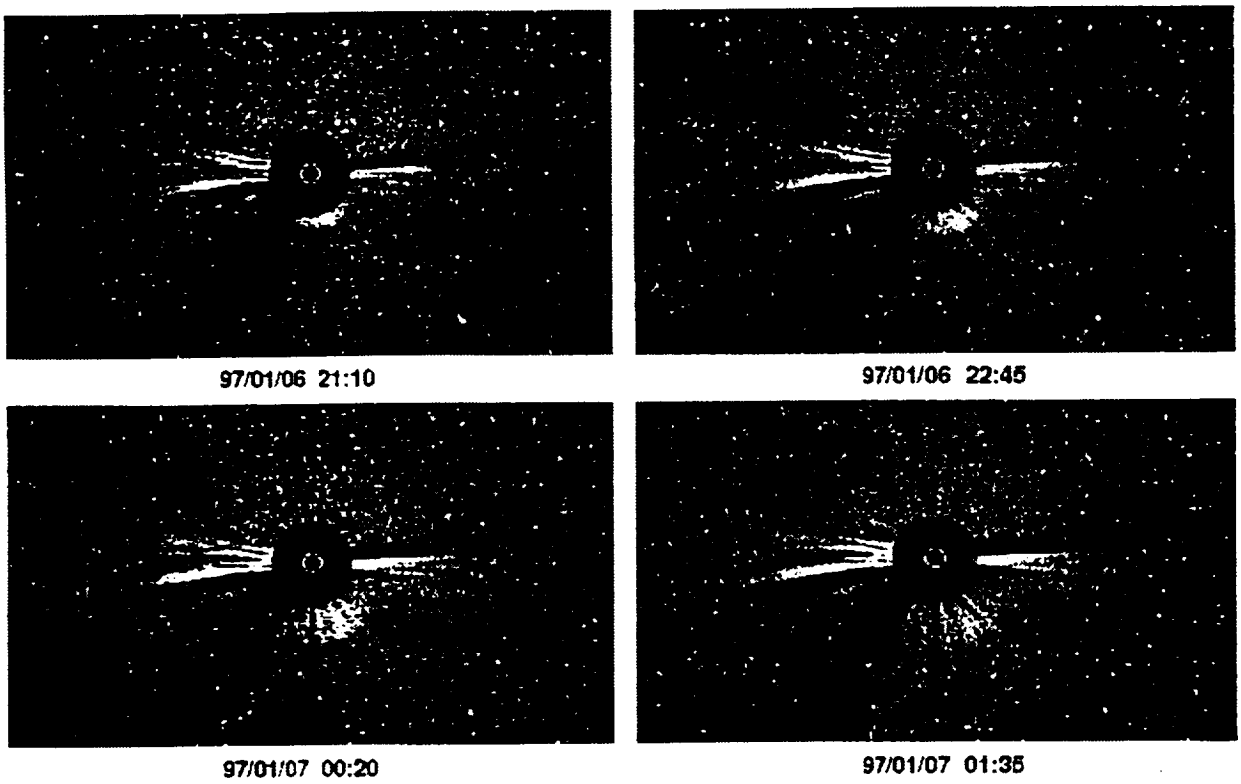

Fig. 4. The partial halo CME of January 6, 1997 observed by the LASCO C3 coronagraph on SOHO. The CME appears as a bright, featureless structure above the South pole (at the bottom of these images). The white circle represents the sun, and the solid disk is the coronagraph occulter, which extends to about 4 $R_\odot$.

dense plug of material was observed at the trailing edge of the magnetic cloud, and Burlaga *et al.* [24] identified this with the filament that was observed to erupt in association with the CME. Wu *et al.* [25] interpreted this event in terms of a streamer and flux rope interaction model for the origin of the CME, and its evolution into a magnetic cloud at 1 AU. This was the first time that a solar eruption was tracked from "cradle to grave," from its onset at the sun, through interplanetary space and its subsequent interaction with the earth.

The Extreme Ultraviolet Imaging Telescope (EIT) [26] on SOHO images the lower corona and solar disk in four narrow spectral bandpasses. EIT is ideally suited to observe the early stages of CMEs and, in combination with LASCO, can be used to identify potentially geoeffective solar eruptions. Fig. 5 shows an eruption in an active region near central meridian, to the north of disk center, that was observed by EIT on May 12, 1997 [27]. The coronal structure at this time was very simple, with just this active region present on an otherwise very quiet disk. Prior to the eruption, the active region appeared as a sigmoid-shaped arcade of loops in the Fe XII 195 A bandpass of EIT. Over a short time (tens of minutes), these loops evolved into a much less sheared arcade almost at right angles to the underlying photospheric magnetic neutral line, and a long-duration flare was recorded by the GOES X-ray detectors. Bright arcades of this type are often seen in association with a CME, straddling the neutral line which was the location of the eruption. Two regions of depleted EUV emission were also observed to form on either side of the newly formed arcade, close to the footpoints of the pre-eruption sigmoid structure. These dimming regions are visible in Fig. 5, and they indicate the evacuation of material from the corona during the event. Also visible in Fig. 5 is the propagation of a large-scale wave disturbance outward from the site of the eruption across almost the entire solar disk. This disturbance is easiest to see in the running difference images in the right column of Fig. 5.

Plunkett *et al.* [28] reported a halo CME in LASCO associated with this event in EIT (Fig. 6). The CME in this case appears all the way round the occulting disk as a ring of excess brightness that moves outward. As with the January 6 event, a moderate geomagnetic storm was reported about 3 days later. Webb *et al.* [29] describe how this event was tracked through interplanetary space as a shock and magnetic cloud, and they interpret the dimming regions observed in EIT as the footpoints of the flux rope that forms the cloud.

The associations between halo CMEs and geomagnetic activity can also be demonstrated on a statistical basis. Brueckner *et al.* [1] found that all halo CMEs observed by LASCO between March 1996 and June 1997 that originated on the visible (front) side of the solar disk were associated with moderate or intense geomagnetic storms. The typical transit time for a disturbance from the sun to earth was about 80 h. Webb *et al.* [30] identified six halos that were likely to be earth-directed in the period from December 1996 to June 1997 and concluded that all six were associated with shocks and magnetic clouds in the solar wind, and moderate geomagnetic storms 3–5 days after leaving the sun. St. Cyr *et al.* [12] performed a more comprehensive statistical study based on LASCO data from January 1996 to April 1998, and concluded that 85% of intense geomagnetic storms (defined as periods when the planetary K_p index reached a value of at least 6) were preceded by front-side halo CMEs.

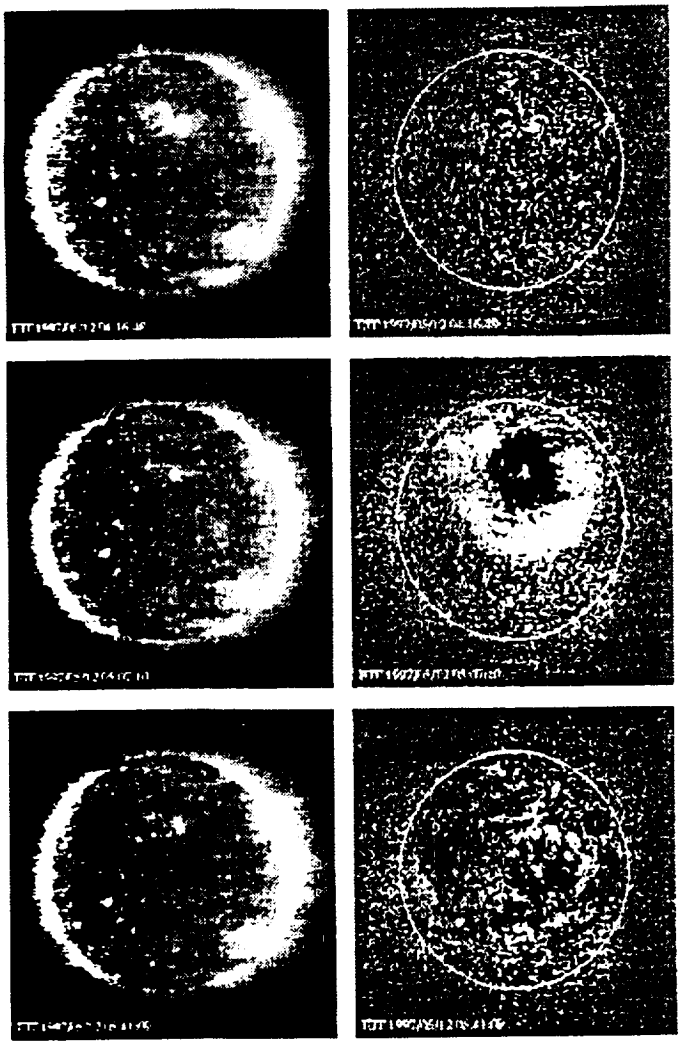

Fig. 5. SOHO EIT observations of the May 12, 1997 CME. The left column is a series of images taken in the Fe XII 195 Å line, showing plasma at approximately 1.5×10^6 K. The right column shows the same images, presented as running differences (each image shows the difference from the previous image in the sequence). The limb of the sun is marked by white circles on the images in the right column.

Fig. 6. The halo CME of May 12, 1997 observed by the LASCO C2 coronagraph on SOHO. This is a difference image, with a pre-event image subtracted. The gray disk represents the occulter, while the location of the sun is indicated by the white circle. The halo appears at rather low contrast above the background, so its location is indicated by arrows to guide the eye.

III. CME Interaction with the Magnetosphere

The most important parameters that determine the geoeffectiveness of a CME are the speed of the ejected solar plasma (the driver gas) and the strength and orientation of the magnetic field (so-called interplanetary magnetic field (IMF)), both within the CME and in the compressed solar wind plasma ahead of it. Gonzalez and Tsurutani [31] demonstrated an empirical relationship between the quantity vB_z and intense magnetic storms (v is the solar wind speed and B_z is the north–south component of the magnetic field). They showed that intense storms are mainly caused by large southward magnetic fields lasting for several hours, often associated with high-speed streams and interplanetary shocks. The energy transfer mechanism between the solar wind and the magnetosphere is primarily magnetic reconnection between southward interplanetary magnetic field and the magnetic field of the earth [32]. The energy transfer efficiency via this mechanism is of the order of 10% during intense storms [33]. Strong southward fields can occur both in the sheath region between the driver gas and the shock and within the coronal ejecta. Another important solar wind parameter used to gauge the occurrence of geomagnetic storms is the dynamic pressure [34], [35]. Most geoeffective CMEs are magnetic clouds in interplanetary space, characterized by high magnetic field strength, low variations in field strength, and large-scale coherent field rotations, often in the north–south direction [2]. Within the sheath region, strong southward fields can be produced by compression and draping of the ambient field over the CME structure [36], [37]. It is important to note that not all fast CMEs are geoeffective. Tsurutani *et al.* [38] showed that five out of six fast CMEs that struck the magnetosphere during 1978–1979 did not produce intense storms, because they lacked strong southward magnetic field components persisting over several hours.

IV. Theoretical Modeling of CMEs Initiation, Propagation, and their Geoeffectiveness

Many investigators have carried out significant theoretical and modeling efforts to reveal the physics of CME initiation, propagation, and their geoeffectiveness. Because of the complexity of the mathematical problem, analytical closed-form solutions are difficult to find. Thus, the theoretical efforts to study the dynamics of CMEs are based on self-consistent numerical magnetohydrodynamic (MHD) simulations. The earlier periods of work done by a number of investigators [39]–[42] focused on the dynamical response of the corona to a thermal pulse introduced at the coronal base. In these studies, the pre-event (initial) states were static coronae with open or closed potential magnetic field topology. The thermal pulse added to this idealized background state was presumed to be released by magneto-to-thermal energy conversion during a flare.

Observations during the mid 1980's showed that CMEs appear to have an earlier onset time than the associated flare [43] and that CMEs seem to be more closely associated with erupting prominences than with flares [44]. Both old and new

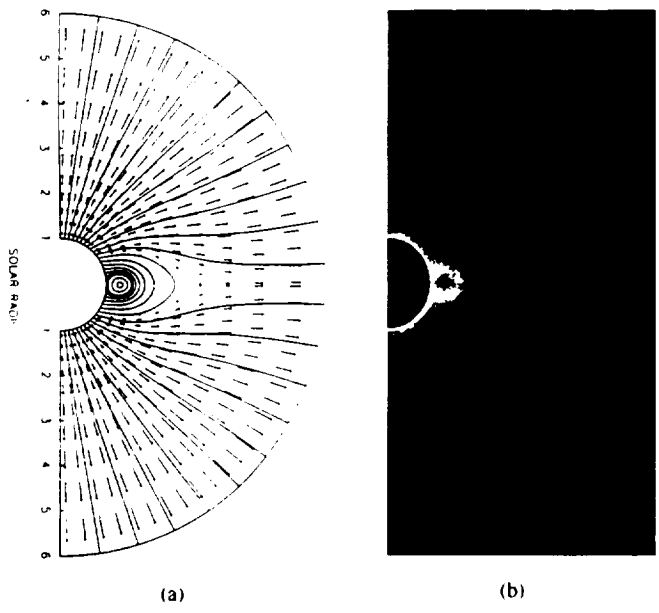

Fig. 7. A representative streamer with cavity magnetic topology where the cavity is formed by a flux-rope with low density and high magnetic field strength. (a) The magnetic field lines and velocity vectors in the meridional plane. (b) The corresponding computed polarization brightness (pB) based on the density distribution of the model [63].

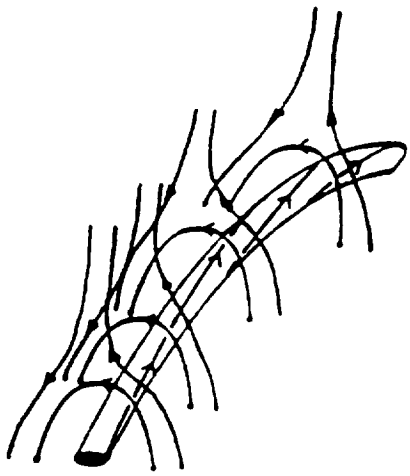

Fig. 8. The schematic description of a three-dimensional view of the streamer arcade system with a filament in it.

observations showed that many CMEs originate from disruption of large-scale quasi-static structures in coronal helmet streamers [45], [9], [46], [18]. Hence, coronal streamers were and are presently considered to be suitable as an initial state to study CME initiation. Steinolfson *et al.* [47] first constructed a self-consistent numerical helmet streamer solution, including the solar wind, using a relaxation method. The importance of the initial corona in CME simulations was soon discovered by Steinolfson and Hundhausen [48]. They constructed three initial coronal models and showed that only the helmet streamer can reproduce the major observed characteristics of looplike CMEs, which consist of a three-part structure: a bright leading edge, dark cavity, and a bright core or kernel [45] similar to the most recent LASCO observation as shown in Fig. 2.

Now it is widely held that CMEs are initiated by the destabilization of large-scale coronal magnetic field structures [9]. But the immediate questions which should be addressed are: 1) what are the solar driver mechanisms which could cause the destabilization of the helmet streamer and 2) what is the energy source that fuels CMEs?

One of the solar driver mechanisms was recognized because of the fact that photospheric shear can store magnetic free energy in the coronal magnetic field. Accordingly, many authors (e.g., [50], [51], [62], [53], [54] demonstrated that photospheric shear (i.e., magnetic field footpoint motion at photospheric level) will cause the coronal helmet streamer to erupt and launch a CME. The emergence of magnetic flux from beneath the photosphere has also been explored as a possible driver mechanism. The addition of new flux causes an increase in the axial electric current in the filament contained within the streamer, thus producing an additional Lorentz force ($\vec{J} \times \vec{B}$) that destabilizes the streamer and initiates a CME [55], [56], [54], [57], [25].

A fundamental theoretical issue of the energy source to fuel CMEs has been discussed in the recent work of Aly [58], [59], Sturrock [60], Low [61] and Low and Hundhausen [62]. Aly [59] and Sturrock [60] showed analytically that if a force-free magnetic field is anchored to the surface of the sun, it cannot have an energy in excess of that in the corresponding fully opened configuration. However, this restriction can be overcome by considering a two-flux system in which a helmet streamer contains a detached magnetic flux rope orthogonal to the streamer axis [61], [62]. The flux rope is theoretically to model a prominence/filament system. The energy in the detached magnetic flux rope is fully available to do work on the plasma by expansion. With the inclusion of gravitational confinement energy resulting from prominence material, the total energy of this system can exceed the open field magnetic energy by an amount comparable to the free energy of the open field configuration, as was demonstrated by a numerical model [63].

Thus, we recognize that it is necessary to employ a more complex MHD model that accounts for the gravitational and magnetic energy of the flux rope, as well as the magnetic energy of the streamer, to study the physics of the two-flux system and its relation to CME initiation and propagation. A numerical MHD model of a coronal streamer consisting of a flux rope [54] with cavity [63] was constructed and verified by observations [57], [18]. The magnetic topology of a representative streamer with cavity is shown in Fig. 7, where the cavity is formed by a flux-rope with low density and high magnetic strength. This type of configuration is commonly observed [18], [46], [49], as shown in Fig. 2. Most recently, Wu *et al.* [64] used this model together with two distinct types of observed CMEs, and they were able to reveal two different types of initiation processes. These are: 1) destabilization of the streamer and flux rope system due to magnetic flux emergence to enhance the electric current of the flux rope and 2) shear induced loss-of-equilibrium of the streamer and flux-rope system to launch a CME. The first process causes the eruption of the flux rope (prominence/filament) prior to the CME, as observed in the January 3, 1998, event [65]. In the second case, the CME is launched prior to the movement of the flux rope

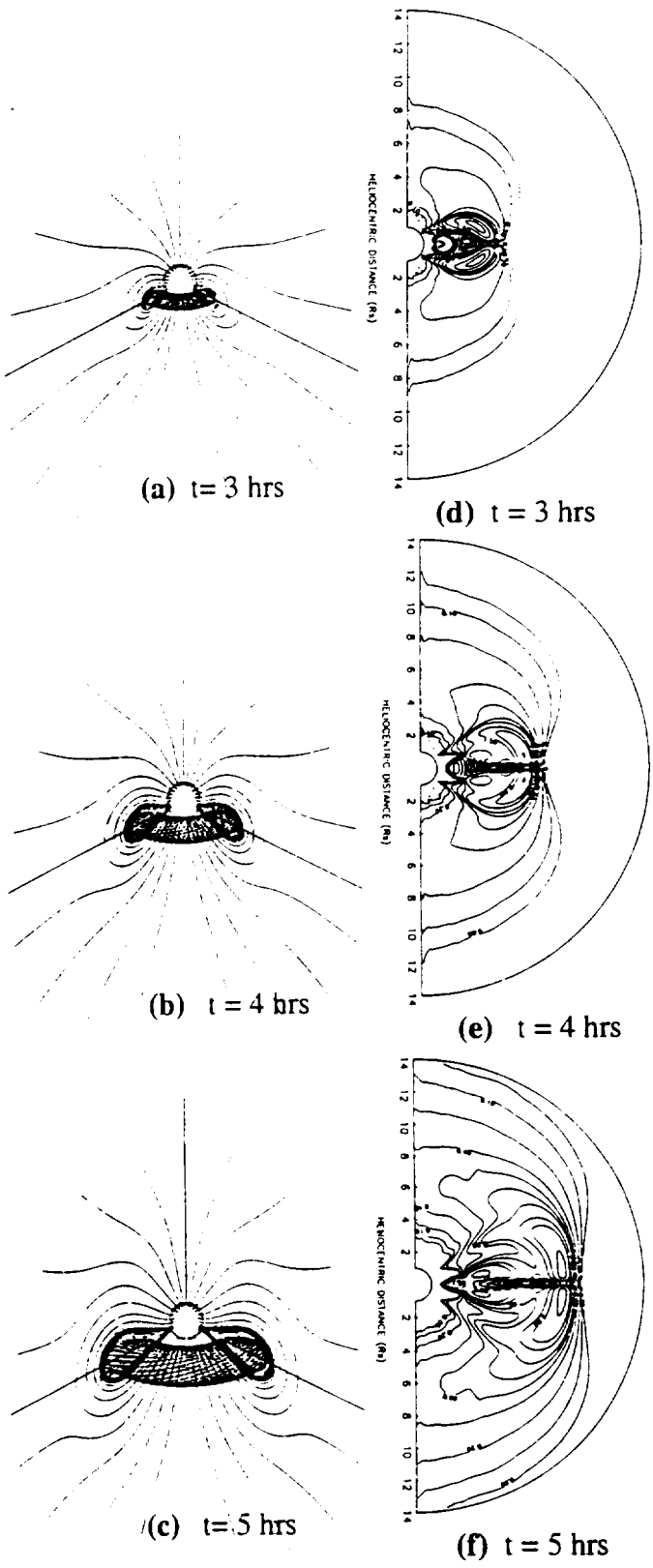

Fig. 9. Evolution of the magnetic field topology of the streamer and flux-rope system as viewed from a vantage point 30 degrees above the equator (a), (b), (c) and the corresponding evolution of the density contours projected in the meridional plane (d), (e), (f) from 1–14 $R_\odot$ (i.e., in the corona) (taken from [25]).

(prominence/filament), as observed in the June 22, 1998 event [65], [66].

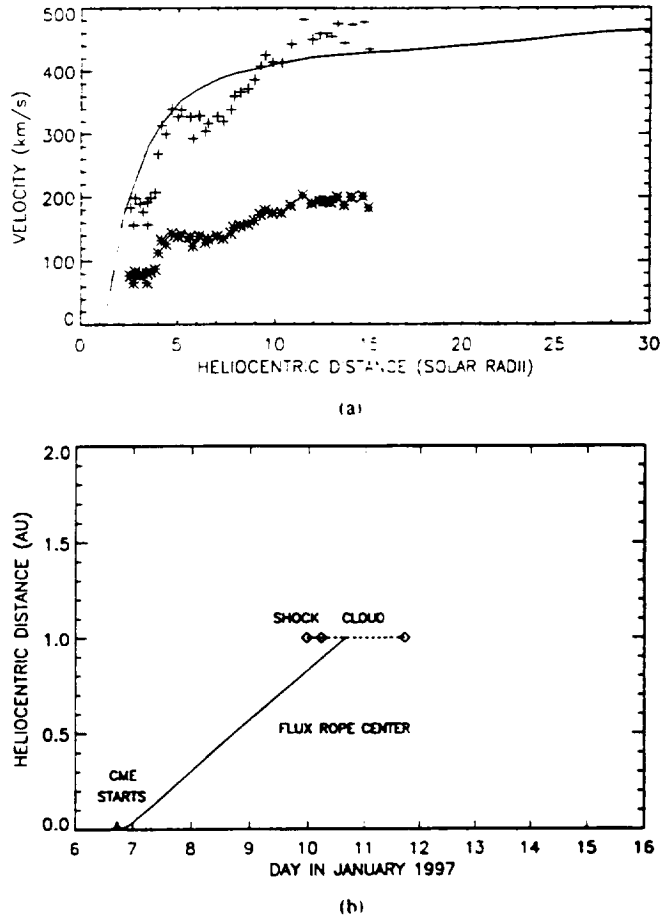

Fig. 10. (a) The computed (—) and measured [plane of sky (* * *) and corrected for projection effect (+ + +)] velocity-height curve in the corona from 1–30 $R_\odot$. (b) the computed height-time curve in the corona from 1–30 $R_\odot$ from the center of the flux-rope, and (c) the computed height-time curve in solar interplanetary space from 1–220 $R_\odot$ from the center of the flux-rope (taken from [25]).

To study the geoeffective CME, we have extended this three-dimensional axisymmetic (commonly known as 2 1/2-D) streamer and flux-rope MHD model to the earth's environment (~220 $R_\odot$). The reason we have chosen this particular model is because it possesses a number of important features of a geoeffective halo CME event observed from January 6–12, 1997 [25].

As discussed earlier, the key parameters that determine the geoeffectiveness of a solar wind structure are the strength and duration of southward IMF and solar wind dynamical pressure at 1 AU (Astronomical Unit ~210 $R_\odot$). As the January 6–12, CME event produced a geomagnetic storm, we use the streamer and flux rope model to determine those two solar wind parameters for this event.

The initial state of this simulation model (i.e., streamer and flux-rope) is given in Fig. 7. Physically, this is a representation of a streamer arcade system with a filament (flux rope) as shown schematically in Fig. 8. The first requirement to have a successful simulation is to match the measured velocity and the time line (i.e., height–time curve) of the event in the corona and interplanetary space. By increasing the strength of the azimuthal component of the flux rope (for details, see [54]), the equilibrium state of the streamer and flux rope system is desta-

TABLE I
THE GLOBAL CONNECTION IS ESTABLISHED BETWEEN THE OBSERVED CME AND MAGNETIC CLOUD FOR THIS SUN–EARTH CONNECTION EVENT

	Propagation Speed (average)	Arrival Time	Duration of Magnetic Cloud (flux-rope) passing
Simulation (flux-rope)	~502 km s^{-1} (at center of flux-rope average v 80 ~ 220 $R_\odot$)	~ 88 hrs	24 hrs
Observation (magnetic cloud)	~ 450 km s^{-1}	~ 92 hrs	24 hrs

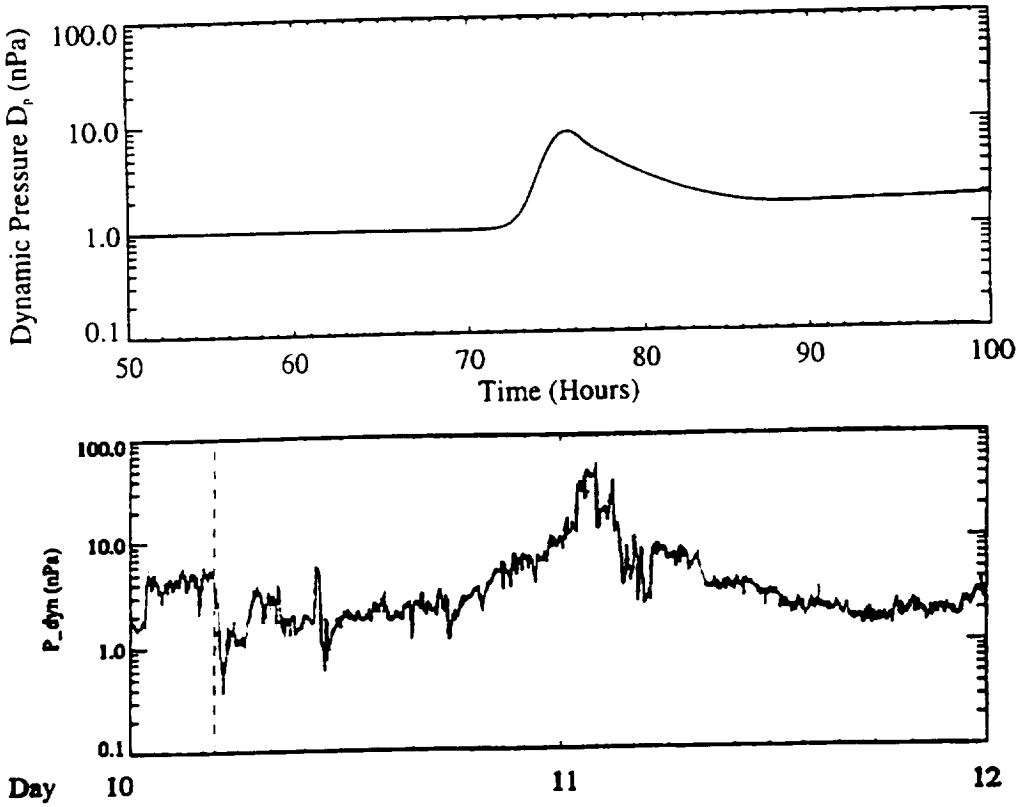

Fig. 11. Computed and measured [35] disturbed solar wind dynamic pressure versus time at 1 AU during the period January 9–12, 1997.

bilized, which launches a CME. The propagation of this newly formed CME in the corona is shown in Fig. 9, and the comparison between the simulated and measured velocity in the corona and time line of CME propagation to 1 AU (Astronomical Unit $\cong 205\ R_\odot$) are shown in Fig. 10. The results given in Fig. 10 and Table I indicate that the simulation and observation are in good agreement. Fig. 9 shows the evolution of the magnetic field topology of the streamer and flux rope system and the corresponding evolution of the density contours projected in the meridional plane from 1 to 14 $R_\odot$ in the corona. The typical three parts of the CME structure can be seen in the density contours $((\rho - \rho_o)/\rho_o)$; a bright loop (i.e., high-density region) followed by a cavity (low-density region) and bright core (flux rope). By looking at the results given in Fig. 9, the halo feature of this event can be readily realized. When the flux rope propagates to 1 AU, it exhibits all the characteristics of a magnetic cloud as demonstrated by a numerical simulation [25]. Using the outputs from the simulation (i.e., magnetic fields, plasma parameters, and velocity of the solar wind), we have computed the dynamical pressure and IMF variations at 1 AU. The comparison with measurements [35], [24] is depicted in Figs. 11 and 12, respectively. These results indicate that the simulation model can be used to establish criteria for geoeffective CMEs.

V. CONCLUSION

The characteristics of CMEs have been documented over three decades of space observation, including three major missions (Skylab, SMM, and SOHO). The rate of occurrence of CMEs varies from about 0.7/day near solar minimum to about 3/day near solar maximum. The corresponding average speed are ~400 km/s, and the fastest events (say, faster than 2000 km/s) are more likely to occur near solar maximum. The total mass per CME is $\sim 10^{16}$ grams, and this does not vary much over the solar cycle. St. Cyr *et al.* [12] present a detailed statistical study of these characteristics using SOHO/LASCO/C2/C3 observations. Even though there are rich observations to deduce these properties, the understanding of the physical mechanisms that cause CMEs are still far from complete. This is because of the lack of measured physical parameters during the initiation phase of the CME. However, using the limited observations and the simulation models [64], two essential physical mechanisms

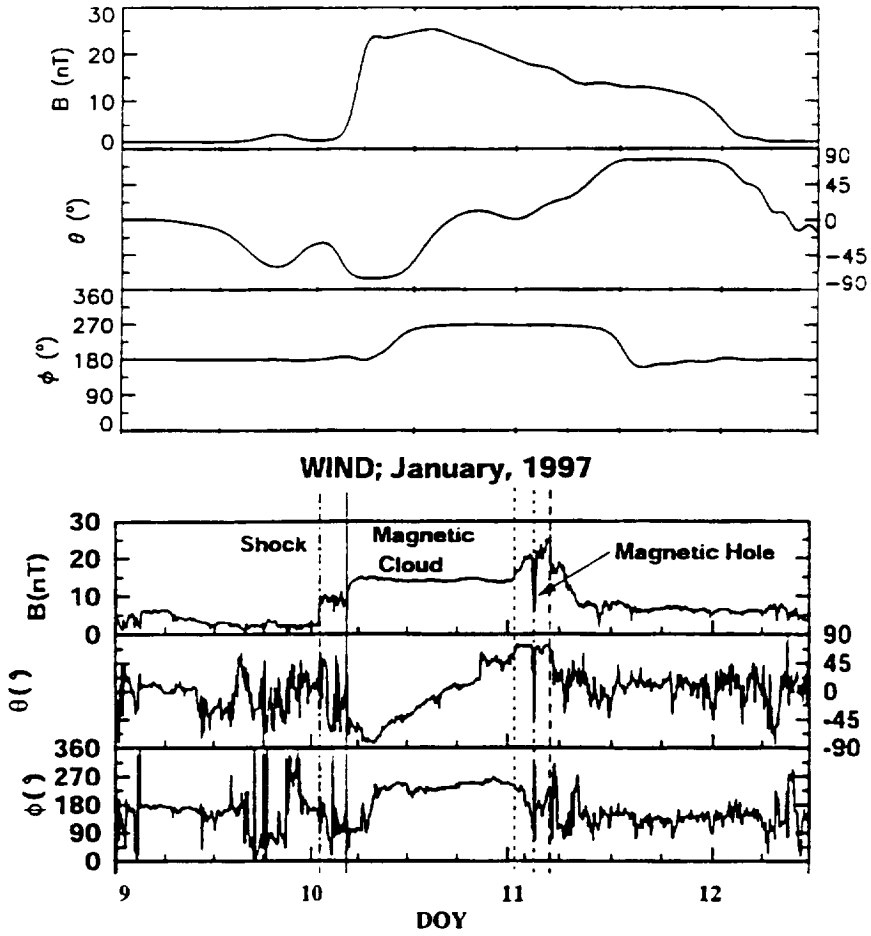

Fig. 12. Computed and Measured [24] disturbed interplanetary magnetic field (IMF) parameters: B is the strength of IMF, the elevation θ and azimuthal ϕ of the IMF direction in the solar ecliptic plane during the period January 9–12, 1997 (reprinted with permission from [25]).

which contribute to the initiation of CMEs can be identified. These are 1) destabilization of a streamer and flux-rope system by magnetic flux emergence, and 2) the photospheric shear-induced loss of equilibrium. It was also demonstrated in this paper that the physical properties of geomagnetically effective CMEs could be deduced from the observations with the aid of simulation models. This could lead to a practical application for the development of a space weather scheme.

REFERENCES

[1] G. E. Brueckner, J.-P. Delaboudiniere, R. A. Howard, S. E. Paswaters, O. C. St. Cyr, R. Schwerin, P. Lamy, G. M. Simnett, B. Thompson, and D. Wang, "Geomagnetic storms caused by coronal mass ejections (CMEs): March, 1996 through June 1997," *Geophys. Lett.*, vol. 25, no. 15, p. 3019, 1998.

[2] L. F. Burlaga, E. Sittler, F. Mariani, and R. Schwenn, "Magnetic loop behind an interplanetary shock: Voyager, Helio, and IMP 8 observations," *J. Geophys. Res.*, vol. 86, pp. 6673–6684, 1981.

[3] D. E. Billings, *A Guide to the Solar Corona*. San Diego, CA: Academic, 1966, p. 65.

[4] R. Tousey, "The solar corona," *Adv. Space Res.*, vol. 13, p. 713, 1973.

[5] J. T. Gosling, E. Hildner, R. M. MacQueen, R. H. Munro, A. I. Poland, and C. L. Ross, "Mass ejections from the sun: A view from Skylab," *J. Geophys. Res.*, vol. 79, pp. 4581–4587, 1974.

[6] ——, "The speeds of coronal mass ejection events," *Solar Phys.*, vol. 48, p. 389, 1976.

[7] R. A. Howard, N. R. Sheeley Jr., M. J. Koomen, and D. J. Michels, "Coronal mass ejections: 1979–1982," *J. Geophys. Res.*, vol. 90, p. 8173, 1985.

[8] J. T. Burkepile and O. C. St. Cyr, "A revised and expanded catalogue of mass ejections observed by the solar maximum mission coronagraph," NCAR/TN-369-STR, 1993.

[9] A. J. Hundhausen, "Sizes and locations of coronal mass ejections: SMM Observations from 1980 and 1984–1989," *J. Geophys. Res.*, vol. 98, p. 13 177, 1993.

[10] A. J. Hundhausen, J. T. Burkpile, and O. C. St. Cyr, "The speeds of coronal mass ejctions SMM observations from 1980 and 1984–1989," *J. Geophys. Res.*, vol. 99, p. 6543, 1994.

[11] R. A. Howard, G. E. Brueckner, O. C. St. Cyr, D. A. Biesecker, K. P. Dere, M. J. Koomen, C. M. Korendyke, P. L. Lamy, A. Llebaria, M. V. Bout, D. J. Michels, J. D. Moses, S. E. Paswaters, S. P. Plunkett, R. Schwerin, G. M. Simnett, D. G. Socker, S. J. Tappin, and D. Wang, "Observations of CMEs from SOHO/LASCO, in coronal mass ejections," in *Geophysical Monograph 99*, 1997, p. 17.

[12] O. C. St. Cyr, R. A. Howard, N. R. Sheeley Jr., S. P. Plunkett, D. J. Michels, S. E. Paswaters, M. J. Koomen, G. M. Simnett, B. J. Thompson, J. B. Gurman, R. Schwerin, D. F. Webb, E. Hildner, and P. L. Lamy, "Properties of coronal mass ejections: SOHO LASCO observations from January 1996 to June 1998," J. Geophys. Res., to be published.

[13] D. Webb and R. A. Howard, "The solar cycle variation of coronal mass ejections and the solar wind mass flux," *J. Geophys. Res.*, vol. 99, p. 4201, 1994.

[14] M. Neugebauer and R. Goldstein, "Particle and field signatures of coronal mass ejections in the solar wind, in coronal mass ejections," in *Geophysical Monograph 99*, 1997, p. 245.

[15] J. T. Gosling, D. J. McComas, J. L. Philips, and S. J. Bame, "Geomagnetic activity associated with earth passage of interplanetary shock disturbances and CMEs," *J. Geophys. Res.*, vol. 96, p. 7831, 1991.

[16] B. T. Tsurutani and R. P. Lin, "Acceleration of greater than 47 keV ions and greater than 2 keV electrons by interplanetary shocks at 1 AU," *J. Geophys. Res.*, vol. 90, p. 1, 1985.

[17] G. E. Brueckner *et al.*, "The large angle coronagraph (LASCO)," *Solar Phys.*, vol. 162, p. 357, 1995.

[18] S. P. Plunkett, A. Vourlidas, S. Simberova, M. Karlicky, P. Kotrc, P. Heinzel, A. Yu. W. P. Kupryakov, Guo, and S.T. Wu, "Simultaneous SOHO and ground-based observations of a large eruptive prominence and coronal mass ejection," *Solar Phys.*, vol. 194, pp. 371–391, 2000.

[19] K. P. Dere, G. E. Brueckner, R. A. Howard, D. J. Michels, and J.-P. Delaboudiniers, "LASCO and EIT observations of helical structure in coronal mass ejections," *Astrophys. J.*, vol. 516, pp. 465–474, 1999.

[20] J. T. Gosling, "Coronal mass ejections and magnetic flux ropes in interplanetary space, in physics of magnetic flux ropes," in *Geophysical Monograph 58*, 1990, p. 343.

[21] R. A. Howard, N. R. Sheeley Jr., M. J. Koomen, and D. J. Michels, "The observation of a coronal transient directed at earth," *Astrophys. J.*, vol. 263, p. L101, 1982.

[22] D. J. Michels, *Proc. of the 5th SOHO Workshop: The Corona and Solar Wind Near Minimum Activity*, 1997, European Space Agency Special Publication, ESA SP-404, p. 567.

[23] D. E. Webb, E. Cliver, N. Gopalswamy, H. Hudson, and O. St. Cyr, "The solar origin of the January 1997 coronal mass ejection, magnetic cloud and geomagnetic storm," *Geophys. Res. Lett.*, vol. 25, p. 2469, 1998.

[24] L. F. Burlaga, E. Sittler, F. Mariani, and R. Schwenn, "A magnetic cloud containing prominence material: January 1997," *J. Geophys. Res.*, vol. 103, p. 277, 1998.

[25] S. T. Wu, W. P. Guo, D. J. Michels, and L. F. Burlaga, "MHD description of the dynamical relationships between a flux-rope, streamer, coronal mass ejection (CME) and magnetic cloud: An analysis of the 1997 January sun–earth connection event," *J. Geophys. Res.*, vol. 104, no. 7, pp. 14 789–14 801, 1999.

[26] J.-P. DeLaboudiniere *et al.*, "EIT: Extreme-utraviolet imaging telescope for the SOHO mission," *Solar Phys.*, vol. 162, p. 291, 1995.

[27] B. J. Thompson, S. P. Plunkett, J. B. Gurman, J. S. Newmark, O. C. St. Cyr, D. J. Michels, and J.-P. Delaboudiniere, "SOHO/EIT observations of an earthward-directed coronal mass ejection on May 12, 1997," *Geophys. Res. Lett.*, vol. 25, p. 2465, 1998.

[28] S. P. Plunkett, K. P. Dere, R. A. Howard, D. J. Michels, G. E. Brueckner, B. J. Thompson, and J.-P. Delaboudiniere, "LASCO/EIT observations of coronal mass ejections from large-scale filament channels, in new perspectives on solar prominences," in *IAU Colloquium 16, ASP Conf. Series*, vol. 150, 1998, p. 475.

[29] D. F. Webb, R.P. Lepping, L. F. Burlaga, C. E. DeForest, D. E. Larson, S. F. Martin, S. P. Plunkett, and D. M. Rust, "The origin and development of the May 1997 magnetic cloud," Geophys. Res. Lett., to be published.

[30] D. F. Webb, E. W. Cliver, N. U. Crooker, O. C. St. Cyr, and B. J. Thompson, "The relationship of halo CMEs, magnetic clouds and magnetic storms," J. Geophys. Res., to be published.

[31] W. D. Gonzalez and B. T. Tsurutani, "Criteria of interplanetary parameters causing intense magnetic storms ($Dst < -100$ nT)," *Planet & Space Sci.*, vol. 35, p. 1101, 1987.

[32] J. W. Dungey, "Interplanetary magnetic field and the auroral zones," *Phys. Rev. Lett.*, vol. 6, p. 47, 1961.

[33] W. D. Gonzalez, B. T. Tsurutani, A. L. C. Gonzalez, E. J. Smith, F. Tang, and S.-I. Akasofu, "Solar wind-magnetosphere coupling during intense magnetic storms (1978–1979)," *J. Geophys. Res.*, vol. 94, p. 8835, 1989.

[34] J. H. Shue, J. K. Chao, H. C. Fu, C. T. Russell, P. Song, K. K. Khurana, and H. J. Singer, "A new functional form to study the solar wind control of the magnetopause size and shape," *J. Geophys. Res.*, vol. 102, no. A5, p. 9497, 1997.

[35] G. D. Lu, N. Baker, R. L. McPherron, C. J. Farrugia, and D. Lummerzheim *et al.*, "Global energy deposition during the January 1997 magnetic cloud event," *J. Geophys. Res.*, vol. 103, no. A6, p. 11 685, 1998.

[36] B. T. Tsurutani, W. D. Gonzalez, F. Tang, S.-I. Akasofu, and E. J. Smith, "Origin of interplanetary southward magnetic fields responsible for major magnetic storms near solar maximum (1978–1079)," *J. Geophys. Res.*, vol. 93, p. 8519, 1988a.

[37] D. J. McComas, J. T. Gosling, S. J. Bame, E. J. Smith, and H. V. Cane, "A test of magnetic field draping induced B_Z perturbations ahead of fast coronal mass ejecta," *J. Geophys. Res.*, vol. 94, p. 1465, 1989.

[38] B. T. Tsurutani, B. E. Goldstein, W. D. Gonzalez, and F. Tang, "Comment on 'A new method of forecasting geomagnetic activity and proton showers' by A. Hewish and P. J. Duffett-Smith," *Planet. & Space Sci.*, vol. 36, p. 205, 1988b.

[39] N. Nakagawa, S. T. Wu, and S. M. Han, "Magnetohydrodynamics of atmospheric transients. I. Basic results of two-dimensional analysis," *Astrophys. J.*, vol. 219, p. 314, 1978.

[40] R. S. Steinolfson, S. T. Wu, M. Dryer, and E. Tandberg-Hanssen, "Magnetohydrodynamic models of coronal transients in the meridional plane. I. The effect of the magnetic field," *Astrophys. J.*, vol. 225, p. 259, 1978.

[41] S. T. Wu, M. Dryer, Y. Nakagawa, and S. M. Han, "Magnetohydrodynamics of atmospheric transients. II. Two-dimensional numerical results for a model solar corona," *Astrophys J.*, vol. 219, pp. 314–323, 1978.

[42] S. T. Wu, Y. Nakagawa, S. M. Han, and M. Dryer, "Magnetohydrodynamics of atmospheric transients. IV. Nonplane two-dimensional analyzes of energy conversion and magnetic field evolution," *Astrophys. J.*, vol. 262, pp. 369–376, 1982.

[43] R. A. Harrison, "Solar coronal mass ejections and flares," *Astron. & Astrophy.*, vol. 162, p. 283, 1986.

[44] S. W. Kahler, "Disruption of a coronal streamer by an eruptive prominence and coronal mass ejection," *Rev. Geophys.*, vol. 25, p. 663, 1989.

[45] R. M. E. Eling and A. J. Hundhausen, "Disruption of a coronal streamer by an eruptive prominence and coronal mass ejection," *J. Geophys. Res.*, vol. 91, p. 10 951, 1986.

[46] K. P. Dere, G E. Bruckner, R. A. Howard, M. J. Koomen, C. M. Korendyke, R. W. Kreplin, D. J. Michels, J. D. Moses, N. E. Moulton, D. G. Socker, O. C. St.Cyr, J. P. Delaboudiniere, G. E. Artzner, J. Brunaud, A. H. Gabriel, J. F. Hochhedez, F. Millier, X. Y. Song, J. P. Chauvineau, J. P. Marioge, J. M. Defise, C. Jamar, P. Rochus, R. C. Catura, J. R. Lemen, J. B. Gurman, W. Neupert, F. Clette, P. Cugnan, E. L. Van Dessel, P. L. Lamy, A. Llebaria, R. Schwenn, and G. M. Simnett, "EIT and LASCO observations of initiation of CMEs," *Solar Phys.*, vol. 174, p. 601, 1997.

[47] R. S. Steinolfson, S. T. Suess, and S. T. Wu, "The steady global corona," *Astrophys. J.*, vol. 255, p. 730, 1982.

[48] R. S. Steinolfson and A. J. Hundhausen, "Density and white light brightness in looplike coronal mass ejections: Temporal evolution," *J. Geophys. Res.*, vol. 93, p. 14 269, 1988.

[49] A. J. Hundhausen, "CME: A summary of SMM observations from 1980 and 1984," in *The Many Faces of the Sun: Scientific Highlights of the SMM*, K. T. Strong, J. L. R. Saba, and B. M. Haisch, Eds: Academic Press, 1989.

[50] Z. Mikic, D. C. Barnes, and D. D. Schnack, "Dynamic evolution of a solar coronal magnetic field arcade," *Astrophys. J.*, vol. 328, p. 830, 1988.

[51] D. Biskamp and H. Wolther, "Magnetic arcade evolution and instability," *Solar Phys.*, vol. 120, p. 49, 1989.

[52] S. T. Wu, M. T. Song, P. C. H. Martens, and M. Dryer, "Shear induced instability and arch filament eruption: A magnetohydrodynamic (MHD) numerical simulation," *Solar Phys.*, vol. 134, pp. 353–377, 1991.

[53] J. A. Linker and Z. Mikic, "Disruption of a helmet streamer by photospheric shear," *Astrophys. J.*, vol. 438, p. L45, 1995.

[54] S. T. Wu and W. P. Guo, "A self-consistent numerical MHD model of helmet streamer and flux rope interactions: Initiation and propagation of coronal mass ejections (CMEs)," in *Geophysical Monograph 99, Coronal Mass Ejections*, N. Crooker, J. Joselyn, and J. Feynman, Eds. Washington, DC: Amer. Geophys. Union, 1997, pp. 83–89.

[55] J. Chen, "Theory of prominence eruption and propagation: Interplanetary consequences," *J. Geophys. Res.*, vol. 101, p. 499, 1996.

[56] J. Chen, R. A. Howard, and G. E. Brueckner, "Evidence of an erupting magnetic flux rope: LASCO coronal mass ejection of 1997 April 13," *Astrophys. J.*, vol. 490, pp. L191–L194, 1997.

[57] S. T. Wu, W. P. Guo, M. D. Andrews, G. E. Brueckner, R. A. Howard, M. J. Koomen, C. M. Korendyke, D. J. Michels, J. D. Moses, D. G. Socker, K. P. Dere, P. L. Lamy, A. Liebana, M. V. Bout, R. Schwenn, G. M. Simnett, D. K. Bedford, and C. J. Eyles, "MHD interpretation of LASCO observations of a coronal mass ejection as a disconnected magnetic structure," *Solar Phys.*, vol. 175, pp. 719–735, 1997.

[58] J. J. Aly, "On some properties of force-free magnetic fields in infinite regions of space," *Astrophy. J.*, vol. 283, p. 349, 1984.

[59] ——, "How much energy can be stored in a three-dimensional force-free magnetic field," *Astrophy. J.*, vol. 375, p. L61, 1991.

[60] P. A. Sturrock, "Minimum energy of semi-infinite magnetic field configurations," *Astrophys. J.*, vol. 380, p. 655, 1991.

[61] B. C. Low, "Magnetohydrodynamic processes in the corona: flares, coronal mass ejections and magnetic helicity," *Plasma Phys.*, vol. 1, p. 1684, 1994.

[62] B. C. Low and J. Hundhausen, "Magnetostatic structures of the solar corona. II. The magnetic topology of quiescent prominences," *Astrophys. J.*, vol. 443, p. 818, 1995.

[63] W. P. Guo and S. T. Wu, "A magnetohydrodynamic description of coronal helmet streamers containing a cavity," *Astrophys. J.*, vol. 494, p. 419, 1998.

[64] S. T. Wu, W. P. Guo, S. P. Plunkett, B. Schmieder, and G. M. Simnett, "Coronal mass ejections (CMEs) initiation: Models and observations," *J. Atmos. Solar Terr. Phys.*, vol. 62, no. 16, p. 1489, 2000.

[65] G. M. Simnett, "The relationship between prominence eruptions and coronal mass ejections," J. Atmos. Solar Terr. Phys., to be published.

[66] B. L. Schmieder, L. van Driel-Gesetelyi, G. Aulanier, P. Demoulin, B. Thompson, G. DeForest, J. E. Wiik, O. C. St. Cyr, G. Simnett, and J. C. Vail, "CMEs and prominences with SOHO, Yohkoh and GBO," Adv. Space Res., to be published.

Simon P. Plunkett received the B.Sc. and Ph.D. degrees in physics from the National University of Ireland. Following completion of his Ph.D. studies in 1991, he was a Research Fellow at the University of Birmingham, UK, until 1996.

He is currently a Research Scientist with the Universities Space Research Association at the Naval Research Laboratory in Washington, DC. His research interests are in the physics of the solar corona, especially coronal mass ejections and their implications for space weather.He is also developing new instrumentation for solar coronal studies on future NASA missions.

Dr. Plunkett is a member of AGU and the Solar Physics Division of the AAS.

Shi Tsan Wu received the B.S. degree from the National Taiwan University, the M.S. degree from the Illinois Institute of Technology, the Ph.D. degree from the University of Colorado.

He yangis a Distinguished Professor of Mechanical and Aerospace Engineering and Director of Center for Space Plasma and Aeronomic Research, The University of Alabama in Huntsville. His research interest include fundamentals of plasmadynamics and magnetohydrodynamics and their application to astrogeophysical flows; numerical simulation on solar energy thermal storage systems; heat exchange design, solar terrestrial environment, laser gasdynamics, hydrodynamics transient; heat transfer, boundary layer type flows, high speed and missile aerodynamics, numerical methods on engineering and physical systems.